33rd Annual International Conference of the IEEE EMBS
Boston, Massachusetts USA, August 30 - September 3, 2011

Propagation Pattern Analysis During Atrial Fibrillation Based on the Adaptive Group LASSO

Ulrike Richter*, Luca Faes, Flavia Ravelli, Leif Sörnmo, *Senior Member, IEEE*

***Abstract*— The present study introduces sparse modeling for the estimation of propagation patterns in intracardiac atrial fibrillation (AF) signals. The estimation is based on the partial directed coherence (PDC) function, derived from fitting a multivariate autoregressive model to the observed signals. A sparse optimization method is proposed for estimation of the model parameters, namely, the adaptive group least absolute selection and shrinkage operator (aLASSO). In simulations aLASSO was found superior to the commonly used least-squares (LS) estimation with respect to estimation performance. The normalized error between the true and estimated model parameters dropped from 0.20±0.04 for LS estimation to 0.03±0.01 for aLASSO when the number of available data samples exceeded the number of model parameters by a factor of 5. The error reduction was more pronounced for short data segments. Propagation patterns were also studied on intracardiac AF data, the results showing that the identification of propagation patterns is substantially simplified by the sparsity assumption.**

I. Introduction

Recent progress indicates that future ablation treatment of atrial fibrillation (AF) should be tailored to the individual patient in order to achieve optimal success rate [1], [2]. Therefore, new methods are required which improve the understanding of AF mechanisms so that the ablation catheter can be accurately guided to the atrial sites which are relevant for terminating the arrhythmia. Methods for propagation pattern analysis are thus of interest as they have the potential to point out ectopic foci and to identify reentrant activities.

Recently, our group proposed the partial directed coherence (PDC) function for propagation pattern analysis during AF, quantifying the causal coupling between multiple signals in the frequency domain [3]. The derivation of the PDC is based on fitting a multivariate autoregressive (MVAR) model to multichannel recordings. Commonly, least-squares (LS) estimation is employed to estimate the MVAR parameters. Improvements in the estimation may be achieved by introducing constraints which encourage sparsity, justified by the observation that connectivity during AF is *a priori* sparse as the coupling between different sites decreases with distance.

Constraints based on the least absolute selection and shrinkage operator (LASSO) [4] have been shown to be particularly effective for estimating sparse models. In the present paper, the adaptive group LASSO (aLASSO) [5] is proposed for improving MVAR modeling of atrial activity during AF. This variant of LASSO allows the construction of groups of unknown parameters which can be pruned jointly. Thus, grouping together MVAR parameters which model coupling from one signal to another should automatically lead to a solution which is sparse with respect to the causal coupling. Obviously, improved accuracy of the MVAR parameter estimates translates to improved accuracy of the PDC.

In the following, details on estimating MVAR models with LS and aLASSO are reviewed. In order to evaluate the impact of the two methods for MVAR parameter estimation on the PDC, simulations are performed. Furthermore, results are presented when the method is applied to AF data acquired with a two-dimensional catheter.

II. Methods

A. Multivariate Autoregressive Modeling

The observations $\mathbf{x}(n) = \begin{bmatrix} x_1(n) & \cdots & x_N(n) \end{bmatrix}^T$, $n = 1, \ldots, T$, obtained simultaneously from N atrial sites, are assumed to be represented by an MVAR model of order m

$$\mathbf{x}(n) = \sum_{k=1}^{m} \mathbf{A}_k \mathbf{x}(n-k) + \mathbf{w}(n), \tag{1}$$

where $\mathbf{A}_k$ is an $N \times N$ matrix comprising the AR parameters $a_{ij}(k)$, $i, j = 1, \ldots, N$, and $\mathbf{w}(n) = \begin{bmatrix} w_1(n) & \cdots & w_N(n) \end{bmatrix}^T$ is a multivariate white noise process with diagonal covariance matrix $\mathbf{\Sigma}_w$, in which each diagonal element σ_{jj}^2 defines the variance of $w_j(n)$.

It is convenient to rewrite (1) in matrix form,

$$\mathbf{X} = \mathbf{Y}\mathbf{B} + \mathbf{W}, \tag{2}$$

where

$$\mathbf{X} = \begin{bmatrix} \mathbf{x}(1) & \cdots & \mathbf{x}(T) \end{bmatrix}^T = \begin{bmatrix} \mathbf{x}_1 & \cdots & \mathbf{x}_N \end{bmatrix},$$
$$\mathbf{W} = \begin{bmatrix} \mathbf{w}(1) & \cdots & \mathbf{w}(T) \end{bmatrix}^T,$$
$$\mathbf{B} = \begin{bmatrix} \mathbf{A}_1 & \cdots & \mathbf{A}_m \end{bmatrix}^T = \begin{bmatrix} \boldsymbol{\beta}_1 & \cdots & \boldsymbol{\beta}_N \end{bmatrix},$$
$$\mathbf{y}(n) = \begin{bmatrix} \mathbf{x}(n) \\ \vdots \\ \mathbf{x}(n-m+1) \end{bmatrix},$$
$$\mathbf{Y} = \begin{bmatrix} \mathbf{y}(1) & \cdots & \mathbf{y}(T) \end{bmatrix}^T.$$

The LS solution for the MVAR parameters is given by [6]

$$\tilde{\boldsymbol{\beta}}_i = \arg\min_{\boldsymbol{\beta}_i} ||\mathbf{x}_i - \mathbf{Y}\boldsymbol{\beta}_i||^2, \tag{3}$$

This work was supported by the Swedish Research Council (#2009-4584).

*U. Richter was with the Signal Processing Group, Department of Electrical and Information Technology, Lund University. She is now with the Department of Experimental Medical Science, Lund University, 22100 Lund, Sweden (e-mail: ulrike.richter@med.lu.se).

L. Faes and F. Ravelli are with the Biophysics and Biosignals Laboratory, BioTech, University of Trento, 38060 Trento, Italy.

L. Sörnmo is with the Signal Processing Group, Department of Electrical and Information Technology and the Center of Integrative Electrocardiology (CIEL), Lund University, 22100 Lund, Sweden.

where $||\cdot||$ denotes the L_2 norm. In order to achieve a sparse solution, certain constraints are introduced in (3). The aLASSO, in which the parameters in $\boldsymbol{\beta}_i$ are divided into L non-overlapping groups $\boldsymbol{\beta}_i^{(l)}$, $l = 1, \ldots, L$, is defined by [5]

$$\hat{\boldsymbol{\beta}}_i = \arg\min_{\boldsymbol{\beta}_i} ||\mathbf{x}_i - \sum_{l=1}^{L} \mathbf{Y}_l \boldsymbol{\beta}_i^{(l)}||^2 \quad (4)$$

$$\text{subject to} \quad \sum_{l=1}^{L} \alpha_{il} ||\boldsymbol{\beta}_i^{(l)}|| \leq t,$$

where $\mathbf{Y}_l$ consists of those columns of $\mathbf{Y}$ that correspond to the parameters contained in $\boldsymbol{\beta}_i^{(l)}$, α_{il} is a positive weighting factor, and t is the upper bound of the constraint.

In the present study, all parameters which model the coupling from one site to another are grouped together such that they can only be pruned jointly, i.e., $\boldsymbol{\beta}_i^{(l)} = \begin{bmatrix} a_{il}(1) & \cdots & a_{il}(m) \end{bmatrix}^T$, $l = 1, \ldots, N$. The corresponding weighting factors have been proposed to adapt to the data when employing the LS solution [5],

$$\alpha_{il} = ||\tilde{\boldsymbol{\beta}}_i^{(l)}||^{-\gamma}, \quad \gamma > 0. \quad (5)$$

B. Model Identification and Selection

The algorithm for least angle regression selection has been employed to solve aLASSO [7]. The algorithm starts with $\hat{\boldsymbol{\beta}}_i^{(l)} = \mathbf{0}$ for all l and approaches in a maximum of L iterations the LS solution, i.e., $\hat{\boldsymbol{\beta}}_i = \tilde{\boldsymbol{\beta}}_i$. In order to select the appropriate iteration step, the Bayesian information criterion (BIC) is employed [5]. For aLASSO, the optimal γ is found by a grid search and determined by the BIC [8]. Finally, the BIC is employed to determine the model order m.

C. Partial Directed Coherence

The PDC from $x_j(n)$ to $x_i(n)$ is given by [3]

$$\pi_{ij}(f) = \frac{\frac{1}{\sigma_{ii}} \bar{A}_{ij}(f)}{\sqrt{\sum_{k=1}^{N} \frac{1}{\sigma_{kk}^2} |\bar{A}_{kj}(f)|^2}}, \quad (6)$$

where $\bar{A}_{ij}(f)$ is an element of $\bar{\mathbf{A}}(f)$, being the Fourier transform of the MVAR model in (1),

$$\bar{\mathbf{A}}(f) = \mathbf{I}_{N\times N} - \sum_{k=1}^{m} \mathbf{A}_k e^{-j2\pi f k}, \quad (7)$$

where $\mathbf{I}$ denotes the identity matrix. The value of the magnitude-squared PDC $|\pi_{ij}(f)|^2$, in the following referred to as PDC, ranges between 0 and 1 and represents the direct coupling strength from $x_j(n)$ to $x_i(n)$ at frequency f, viewed in relation to the direct coupling strength of $x_j(n)$ to all other signals $x_k(n)$, $k \neq i$.

During AF, the PDC is of special interest in an interval centered around the dominant frequency (DF) of the source $x_j(n)$. Thus, the integrated PDC is defined by [3]

$$\Pi_{ij}^2 = \frac{1}{2\Delta f} \int_{f_0-\Delta f}^{f_0+\Delta f} |\pi_{ij}(f)|^2 df, \quad (8)$$

where f_0 denotes the DF, corresponding to the highest peak in the 3–12 Hz range of the auto-spectrum of $x_j(n)$, and Δf determines the width of the integration interval.

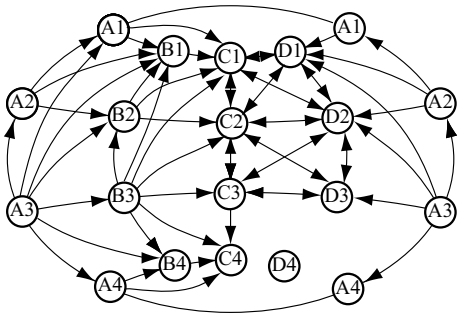

Fig. 1. Projection of the sphere employed in the simulations illustrating the positions of the recording sites and the propagation pattern as imposed by the binary connectivity matrix $\mathbf{C}$. The propagation originates at site A3, and a more disorganized region of propagation was defined at sites C1, C2, C3, D1, D2, and D3, while D4 was left isolated.

D. Surrogate Data Testing

Surrogate data testing is performed for the integrated PDC by computing Π_{ij}^2 for both the original time series $\mathbf{x}(n)$ and M surrogate time series $\mathbf{y}^{(l)}(n)$, $l = 1, \ldots, M$ [3]. Each $\mathbf{y}^{(l)}(n)$ is computed specifically for the causal coupling under investigation such that there is no direct causal coupling from $y_j^{(l)}(n)$ to $y_i^{(l)}(n)$. The integrated PDC calculated from the original time series is considered significant if its value exceeds the 95th percentile of the distribution of corresponding values obtained from the surrogate data sets.

III. Database

A. Simulations

Based on the MVAR model in (1) a number of simulations were carried out for the geometry of a sphere with $N = 16$ recording sites. The sites were distributed along four lines of longitude, A to D, situated at 0°, 90°, 180°, and 270°, respectively. Four evenly spaced bipolar electrodes were placed at each longitude and denoted A1 to A4, ..., D1 to D4.

In a first step, a propagation pattern was imposed by defining an $N \times N$ binary connectivity matrix $\mathbf{C}$ such that $C_{ij} = 1$ when propagation was allowed from site j to i, and $C_{ij} = 0$ otherwise, except $C_{ii} = 1$, see Fig. 1. In a second step, each direct coupling from site j to i was assigned a probability which decreased with distance [9],

$$P_{ij} = \exp\left(-\frac{d_{ij}^2}{\lambda^2}\right), \quad (9)$$

where d_{ij} is the distance between recording sites i and j determined for a sphere with unit radius, and the decrease rate is controlled by $\lambda \geq 0$, here chosen to $\lambda = 1.5$. Thus, direct coupling from site j to i was present when $C_{ij} = 1$ as well as $\delta_{ij} \geq 1 - P_{ij}$, where δ_{ij} was a uniformly distributed random variable, $\mathcal{U}(0, 1)$. For the chosen settings, 42 out of the $N^2 = 256$ possible direct couplings became non-zero. In the final step, the MVAR parameters corresponding to the direct couplings were determined for model order $m = 3$. The MVAR parameters $a_{ii}(k)$ were determined such that the MVAR process resembled the preprocessed

AF signals, i.e., with narrowband characteristics. Complex conjugated pole pairs $p_{1/2}^{(i)} = r_0 e^{\pm \iota \phi_0}$, $i = 1, \ldots, N$, were defined by choosing the radius r_0 and the angle ϕ_0 from $\mathcal{U}(0.5, 0.6)$ and $\mathcal{U}(0.9, 1.1) \cdot \pi/4$, respectively. Additional real poles $p_3^{(i)}$, $i = 1, \ldots, N$, were chosen from $\mathcal{U}(0.1, 0.3)$. The remaining parameters $a_{ij}(k)$, $i \neq j$, were sampled from a normal distribution $\mathcal{N}(0, 0.5)$. Furthermore, employing $\mathbf{\Sigma}_w = \mathbf{I}_{N \times N}$, the non-zero integrated PDCs Π_{ij}^2, which in the simulations were calculated by integrating $|\pi_{ij}(f)|^2$ over the entire frequency range, yielded 0.38±0.29.

Accuracy of the estimation methods is evaluated with the normalized error function

$$\varepsilon(\mathbf{M}) = \frac{||\mathbf{M} - \hat{\mathbf{M}}||^2}{||\mathbf{M}||^2}, \tag{10}$$

and is employed for both the MVAR parameters, i.e., $\mathbf{M} = \mathbf{B}$, and the integrated PDC, i.e., $\mathbf{M} = \mathbf{\Pi}^2$, which is an $N \times N$ matrix comprising the different Π_{ij}^2.

B. AF Recordings

The method is illustrated on a recording acquired from a patient with paroxysmal AF who underwent an electrophysiological study with a multi-electrode basket catheter (Constellation catheter, EP Technologies, Boston Scientific) in the right atrium (RA). The basket catheter consisted of eight splines, A to H, each carrying eight evenly spaced electrodes. Thirty-two bipolar intracardiac electrograms were acquired by coupling adjacent pairs of electrodes (CardioLab System, 30–500 Hz [Prucka Engineering, Inc.]). The sampling rate was 1 kHz, and one 5-s segment was chosen for analysis.

The electrograms were preprocessed with bandpass filtering (finite impulse response (FIR), 40–250 Hz), rectification, and lowpass filtering (FIR, 0–20 Hz) [3]. This preprocessing results in signals with an amplitude proportional to the high-frequency components (40–250 Hz), which correspond to the rapid changes in amplitude characteristics of the atrial activations. Finally, the sampling rate was decimated to 100 Hz.

IV. Results

Based on the above simulation model, 20 simulations were carried out for sample sizes $T = 5mN$, $3mN$, and $2mN$. For the AF recordings, the optimal model order was searched for in the interval [1,15], the number of surrogate time series was set to $M = 100$, and the integrated PDC was obtained for $\Delta f = 0.5$ Hz.

A. Simulations

The normalized error functions $\varepsilon(\mathbf{B})$ and $\varepsilon(\mathbf{\Pi^2})$ are displayed in Figs. 2(a) and (b), respectively. The results show that aLASSO performs much better in estimating the MVAR model and the integrated PDC than does LS estimation for all three sample sizes T. Furthermore, the improvement in estimation accuracy can be seen to increase with decreasing sample size.

B. AF Recordings

The estimated model order was $\hat{m} = 4$. The percentage of significant direct couplings between different sites decreases slightly from 8.6% in LS estimation to 8% for aLASSO. The corresponding Π_{ij}^2 ranges from 0.05 to 0.41 (0.11±0.06) in LS estimation and from 0.0001 to 0.52 (0.12±0.11) in aLASSO.

The propagation pattern derived from LS estimation is rather difficult to interpret, see Fig. 3(a). A clearer manifestation of the propagation pattern is provided by the directed graph derived from aLASSO, see Fig. 3(b), which suggests a propagation originating from the low septal RA close to sites EF3 and EF4. From there, the electrical activity propagates caudocranially in the septal RA as well as transversely towards the anterior and posterior RA. In the posterior/posterolateral wall, craniocaudal propagation is indicated, and finally, the propagation spreads towards the lateral RA from both anterior and posterolateral regions.

V. Discussion

Successful estimation of the MVAR parameters is crucial for successful estimation of the PDC, since the calculation of the PDC is derived from the model parameters. In order to incorporate prior information on sparsity of the solution aLASSO was proposed, which stands in contrast to LS estimation in which "full" connectivity is implicitly assumed. In detail, aLASSO improves the estimation by introducing a constraint on the LS solution which is defined as an intermediate between the L_1 and L_2 norm. While the L_2 norm is responsible for avoiding overfitting, the singularities caused by the L_1 norm achieve sparsity. The sparsity of the resulting solution can for the analysis of intracardiac AF recordings be motivated by the observation that direct couplings over longer distances are likely to be zero.

Previously, other LASSO variants such as the ordinary LASSO and group LASSO have been employed for MVAR estimation, e.g., when analyzing the functional connectivity between different brain areas [9], [10]. In those studies, the main interest was the detection of directed information flow based on tests applied directly to the MVAR parameters. In the present work, the accuracy of the estimated MVAR parameters is also of interest, as they are used in the calculation of the PDC. From a number of simulations based on the MVAR model, aLASSO leads to major improvements in estimation accuracy of the MVAR model as well as the PDC when compared to LS estimation.

The method has been evaluated on a 5-s segment of a recording acquired in the RA during paroxysmal AF. For LS estimation, a large number of significant direct couplings were present over longer distances, leading to difficulties in the identification of the propagation pattern from the corresponding directed graph. The interpretation of the directed graph was substantially simplified by the sparsity achieved with aLASSO. A propagation starting in the low septal RA was evidenced, suggesting atrial impulses entering the RA from the left atrium at the coronary sinus ostium. This RA breakthrough site as well as the subsequent

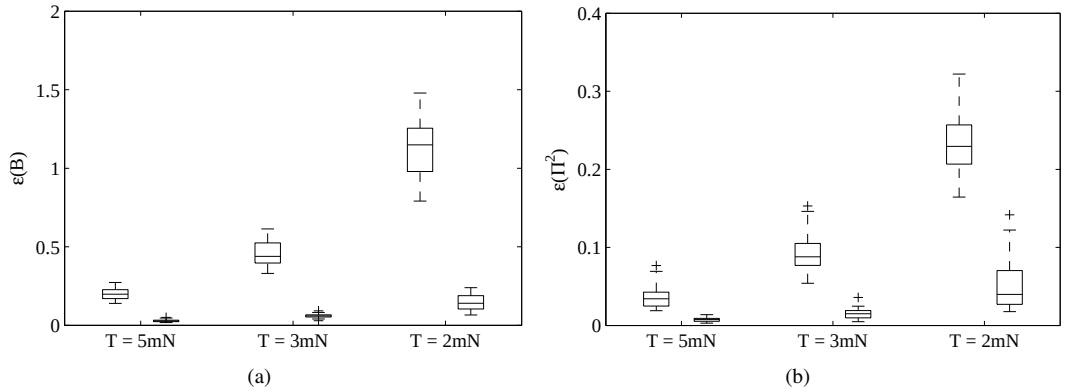

Fig. 2. The normalized error function for (a) $\mathbf{B}$ and (b) $\mathbf{\Pi}^2$ for different sample sizes T. For each T, results are presented for LS estimation and aLASSO, to the left and right, respectively. The lines of the boxes correspond to (from top to bottom) the upper quartile, the median, and the lower quartile.

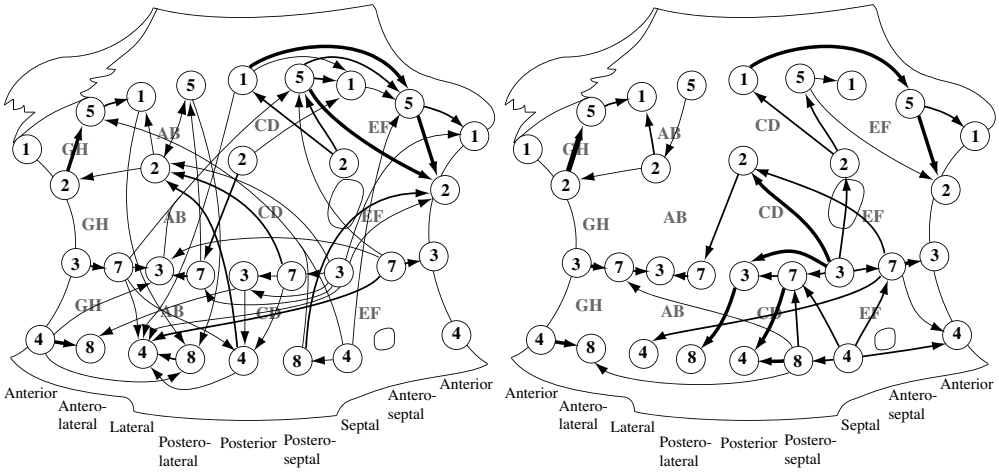

Fig. 3. Directed graphs illustrating the propagation pattern during one 5-s segment of AF based on (a) LS estimation and (b) aLASSO. Only direct couplings corresponding to Π^2_{ij} which are significant and ≥ 0.05 are displayed. The arrow width is proportional to the size of the corresponding Π^2_{ij}.

propagation pattern agrees with clinical observations [11], which highlights the potential of the PDC as a method for extracting information on the propagation patterns during AF.

VI. Conclusions

In the present paper, the estimation of propagation patterns in intracardiac AF signals in terms of the PDC has been shown to be substantially improved when prior information on sparsity is incorporated in the underlying model. The method may serve as a support for the electrophysiologist when manual evaluation of the recorded signals is difficult.

References

[1] K. Nademanee, J. McKenzie, E. Kosar, M. Schwab, B. Sunsaneewitayakul, T. Vasavakul, C. Khunnawat, and T. Ngarmukos, "A new approach for catheter ablation of atrial fibrillation: mapping of the electrophysiologic substrate," *J. Am. Coll. Cardiol.*, vol. 43, pp. 2044–2053, 2004.

[2] H. Oral, A. Chugh, E. Good, S. Sankaran, S. S. Reich, P. Igic, D. Elmouchi, D. Tschopp, T. Crawford, S. Dey, A. Wimmer, K. Lemola, K. Jongnarangsin, F. Bogun, F. Pelosi, and F. Morady, "A tailored approach to catheter ablation of paroxysmal atrial fibrillation," *Circulation*, vol. 113, pp. 1824–1831, 2006.

[3] U. Richter, L. Faes, A. Cristoforetti, M. Masè, F. Ravelli, M. Stridh, and L. Sörnmo, "A novel approach to propagation pattern analysis in intracardiac atrial fibrillation signals," *Ann. Biomed. Eng.*, vol. 39, pp. 310–323, 2010.

[4] R. Tibshirani, "Regression shrinkage and selection via the lasso," *J. Roy. Statist. Soc. Ser. B*, vol. 58, pp. 267–288, 1996.

[5] H. Wang and C. Leng, "A note on adaptive group lasso," *Comp. Stat. Data Analysis*, vol. 52, pp. 5277–5286, 2008.

[6] H. Lütkepohl, *New Introduction to Multiple Time Series Analysis*. Springer-Verlag Berlin Heidelberg, 2005.

[7] M. Yuan and Y. Lin, "Model selection and estimation in regression with grouped variables," *J. Roy. Statist. Soc. Ser. B*, vol. 68, pp. 49–67, 2006.

[8] G. Schwarz, "Estimating the dimension of a model," *Ann. Stat.*, vol. 6, pp. 461–464, 1978.

[9] P. A. Valdés-Sosa, J. M. Sánchez-Bornot, A. Lage-Castellanos, M. Vega-Hernández, J. Bosch-Bayard, L. Melie-García, and E. Canales-Rodríguez, "Estimating brain functional connectivity with sparse multivariate autoregression," *Phil. Trans. Roy. Soc. Lond. B Biol. Sci.*, vol. 360, pp. 969–981, 2005.

[10] S. Haufe, R. Tomioka, G. Nolte, K.-R. Müller, and M. Kawanabe, "Modeling sparse connectivity between underlying brain sources for EEG/MEG," *IEEE Trans. Biomed. Eng.*, vol. 57, pp. 1954–1963, 2010.

[11] S. Saksena, N. D. Skadsberg, H. B. Rao, and A. Filipecki, "Biatrial and three-dimensional mapping of spontaneous atrial arrhythmias in patients with refractory atrial fibrillation," *J. Cardiovasc. Electrophysiol.*, vol. 16, pp. 494–504, 2005.